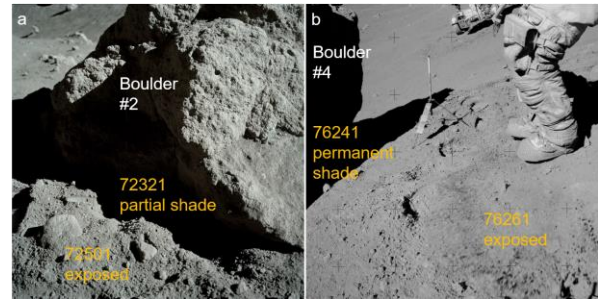


**NANOSCALE INSIGHTS INTO APOLLO 17 REGOLITH SAMPLES FROM STATIONS 2 AND 6: EXPOSURE HISTORY, MINERAL PHASE COMPOSITION, AND SPACE WEATHERING.** B. A. Cymes<sup>1</sup>, K. D. Burgess<sup>2</sup>, R. M. Stroud<sup>2</sup>, and The ANGSA Science Team, <sup>1</sup>NRC Postdoctoral Research Associate, U.S. Naval Research Laboratory, Washington DC 20375 (brittany.cymes.ctr@nrl.navy.mil), <sup>2</sup>U.S. Naval Research Laboratory, Washington DC 20375.

**Introduction:** Solar wind irradiation and micrometeoroid bombardment are the dominant space weathering processes on the Moon. They alter the surfaces of regolith grains, often producing thin (<200 nm) amorphous rims that can be enriched in vesicles, nanophase metallic iron inclusions (npFe<sup>0</sup>), or a combination of these [1-3]. Two variables which remain unconstrained among the factors that influence the formation of these features are recent exposure history and mineral phase composition. To address knowledge gaps regarding systematic differences in the character of space weathered rims in the context of exposure history and composition, we analyzed regolith samples from the Apollo 17 mission using scanning transmission electron microscopy (STEM), electron energy loss spectroscopy (EELS), and energy dispersive spectroscopy (EDS). These advanced microanalytical techniques can reveal these fine scale features to help constrain space weathering histories at the individual grain scale. The efforts described here are part of a broad initiative to evaluate samples from the ‘new’ lunar collection – to which these samples will be compared – as part of the Apollo Next Generation Sample Analysis (ANGSA) program.

**Methods:** The samples analyzed were soils 72321 and 72501 collected from the foot of the South Massif (St. 2) representing mature ( $I_S/FeO = 73, 81$ ), partially shaded and exposed conditions, respectively (Fig. 1a), and soils 76241 and 76261 from the south slope of the North Massif (St. 6) representing submature ( $I_S/FeO = 56, 58$ ), permanently shaded and exposed conditions, respectively (Fig. 1b). The samples were prepared for STEM analysis by embedment in superglue-tipped epoxy blocks and ultramicrotome sectioning. Sections were loaded onto 3.0 mm lacey C-substrated Cu grids and held under vacuum at room temperature for at least 48 hours to drive off adsorbed water before introduction to the UHV system. The EELS and EDS data were acquired using the Nion UltraSTEM200-X at the U.S. Naval Research Laboratory, which is equipped with a Gatan Enfium ER EEL spectrometer and a Bruker SDD-EDS detector. The STEM was operated at 200 keV with a ~0.1 nm probe. The EEL spectra were collected as spectrum images (SI), in which a spectrum is collected at each pixel allowing for spatial visualizations of composition, oxidation state, and specimen thickness variations.



**Figure 1.** (a) Location of partially shaded and exposed samples from station 2 (NASA photo #AS17-137-20925). (b) Location of permanently shaded and exposed samples from station 6 (NASA photo AS17-141-21605).

**Results and Discussion:** Anorthite and glass are the most abundant phases observed with minor olivine, ilmenite, and Ca-pyroxene, consistent with prior work [4]. The majority of the space weathered rims are generally <150 nm thick and bear abundant npFe<sup>0</sup> typically 3-15 nm in diameter with a few individuals in the 25-50 nm range; vesicular rims are less common. Geochemically, Fe-rich rims in Ca plagioclase and ilmenite are often associated with adjacent enrichment in Mg (Fig. 2 a-b) and Fe-rich rims in olivine have been observed to be Mg-poor (Fig. 2c), a characteristic potentially related to preferential weathering of adjacent Mg-rich material and subsequent vapor deposition. Several novel rim features have also been observed, including vesicular npFe<sup>0</sup>, oxidized npFe<sup>x</sup>, and some unique melt-derived features. Further analysis is required to link geochemical and textural characteristics to exposure history; however, vesicular npFe<sup>0</sup> – for example – have only been observed in samples with full or partial exposure. This relationship is significant because He has been detected within ‘pockets’ in two vesicular npFe<sup>0</sup> particles in sample 72501 via EELS-SI as shown in Figure 3 where the He K-edge is visible above the silica plasmon. Helium is one of the main components of solar wind and has been observed previously in vesicular space-weathered material [5], a challenging feat given its volatility. This unique relationship with npFe<sup>0</sup> may shed light on the emplacement and cycling of He within the regolith. In order to facilitate He and potential H detection moving forward, we plan to utilize a specialized cold stage in a

focused ion beam microscope in order to slow diffusion and mitigate potential loss during sample preparation.

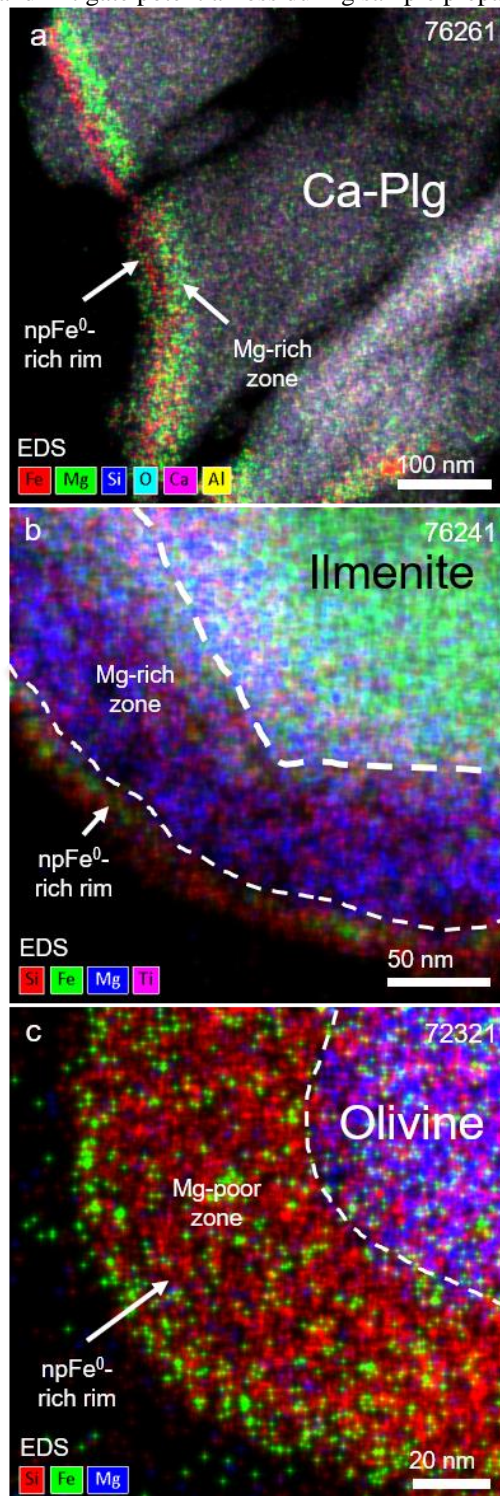


**Figure 2.** (a) EDS map of a plagioclase crystal with an Mg-rich zone associated with an npFe<sup>0</sup>-rich rim. (b) EDS map of an ilmenite crystal with an Mg-rich zone associated with an npFe<sup>0</sup>-rich rim. (c) EDS map of an olivine crystal with a Si and npFe<sup>0</sup>-rich rim.

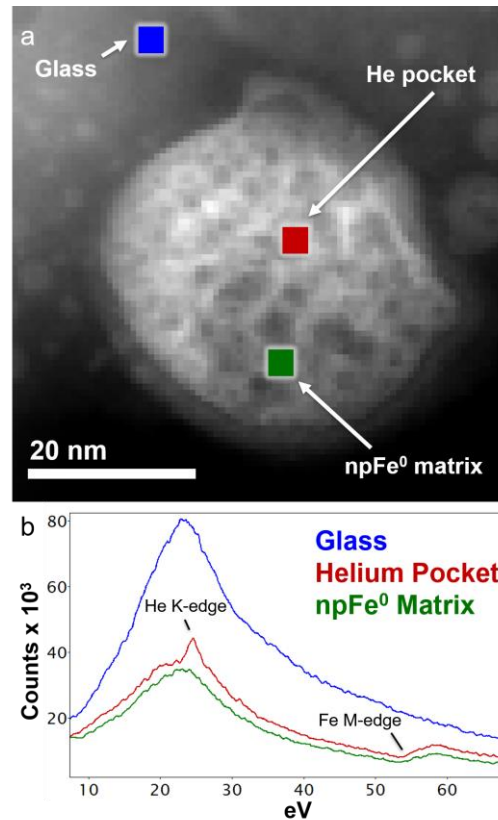


**Figure 3.** (a) EELS-SI of a vesicular npFe<sup>0</sup> particle with spectrum-extraction windows indicated. (b) EEL spectra of the selected windows showing the He K-edge compared to the glass and npFe<sup>0</sup> matrices.

**Conclusion:** This investigation explores lunar soils curated at room temperature to be later compared with new frozen samples as a part of the ANGSA initiative. The data collected thus far reflect a complex material that has preserved nuanced, fine scale textural and chemical characteristics that may be useful in the evaluation of the individual and tandem influences of solar wind irradiation and micrometeoroid bombardment in the development of lunar space weathered rims. These efforts may also shed light on phenomena such as lunar swirls and provide reference data for further lunar exploration missions and investigations of space weathering on other airless bodies.

**Acknowledgments:** This work was supported by NASA award 80HQTR19T0057 and SSERVI award 80NSSC19M0215.

**References:** [1] Pieters, C. M. and Noble, S. K. (2016) *J. Geophys. Res.* 121, 1865-1884. [2] Hapke, B. (2001) *J. Geophys. Res.* 106, 10039-10073. [3] Keller, L. P. and McKay, D. S. (1997) *Geochim. Cosmochim. Acta* 61, 2331-2341. [4] Heiken, G. and McKay, D. S. (1974) *LPSC Proc.*, 5, 843-860. [5] Burgess, K. D. and Stroud, R. M. *Geochim. Cosmochim. Acta* 224, 64-79.